

Optimisation of photoacoustic resonant cells with commercial microphones for diode laser gas detection

V.A. Kapitanov^a, V. Zeninari^{b,*}, B. Parvitte^b, D. Courtois^b,
Yu.N. Ponomarev^a

^a *Institute of Atmospheric Optics of SBRAS, 1 Akademicheskii Ave., Tomsk 634055, Russia*

^b *Groupe de Spectrométrie Moléculaire et Atmosphérique (GSMA), UMR CNRS 6089, Faculté des Sciences, BP 1039, F-51687 Reims Cedex 2, France*

Abstract

The theoretical and experimental study of the differential Helmholtz resonant (DHR) cell sensitivity under variation of the total gas pressure is made for various commercial microphones. Near-infrared lasers (room-temperature diode lasers) were used to measure the response of DHR cell versus pressure of the absorbing gas and frequency of the laser radiation modulation. Several molecular absorbers like H₂O, CH₄, mixed with molecular buffer gases were used to investigate the behavior of the photoacoustic (PA) signal characteristics with a DHR cell. The experimental data are compared with the results of computer simulation. The minimal detectable concentrations of gases were determined for the DHR cell for each commercial microphone. © 2002 Elsevier Science B.V. All rights reserved.

Keywords: Photoacoustic gas detection; Helmholtz resonator; Infrared spectrometer

1. Introduction

The photoacoustic (PA) spectroscopy based on the PA effect has been identified as an ultra-sensitive technique [1]. The PA technique consists of sending chopped radiation into a sample gas cell containing a microphone. Any absorbed radiation will be, in general, converted to thermal motion of the gas by intermolecular processes thus leading to a modulated pressure wave detectable with a

microphone. For low concentrations, the PA signal is proportional to the product of the response of the cell, the microphone sensitivity, the laser power and the absorption coefficient of the gas.

In the range of pressures close to one atmosphere, the spectral lines broadening by pressure induces essential limits on the spectral selectivity of the method. This is of particular importance in the spectral ranges, where significant absorption by molecules of main atmospheric gases, such as the water vapour and CO₂, takes place. At the reduced pressure P in the PA cell, the line width decreases proportionally to $\sim P$, and the possibility appears to distinguish the absorption lines of pollutants from those of main atmospheric components. Within the pressure range $\sim 10^4$ Pa, the

* Corresponding author. Tel.: +33-3-2691-3445; fax: +33-3-2691-3147

E-mail address: virginie.zeninari@univ-reims.fr (V. Zeninari).

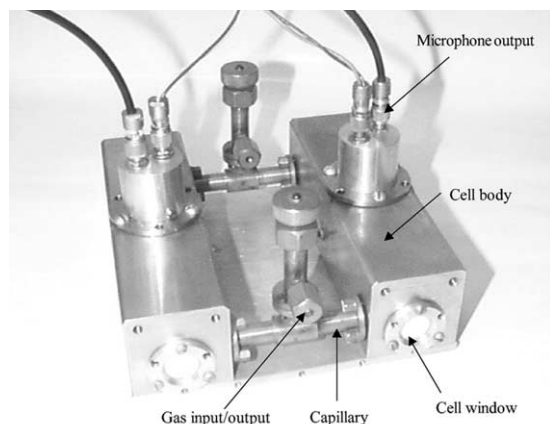


Fig. 1. Photoacoustic (PA) detector with differential Helmholtz resonant (DHR) cell.

density decrease of the gas under measurement is compensated by the spectral line narrowing, therefore the decrease of the absorption coefficient in the line centre becomes insignificant, i.e. of the order of 30–50%.

The magnitude of the ultimate sensitivity of the PA-spectrometer–gas-analyser

$$(k_v)_{\min} = (\sigma_v \cdot c_{\min}) = \frac{\sqrt{U_n^2}}{R_c \cdot R_m \cdot W_0} \quad (1)$$

at atmospheric pressure is mainly determined by characteristics of the acoustic resonator. Here σ_v ,

is the absorption cross-section, c_{\min} is the minimal detectable concentration of pollutants, $\sqrt{U_n^2}$ is a r.m.s. value of noise intensity at the preamplifier input, R_c is the resonant cell sensitivity, R_m is the microphone sensitivity, and W_0 is the power of laser source.

This paper presents the results of theoretical and experimental studies of sensitivity of the resonant PA differential Helmholtz resonant (DHR) detector applied to detection of trace gases in the atmosphere, as well as the spectroscopy of flowing gas in PA cells of flow and flowless type at reduced pressure.

2. Design of PA DHR cell

The high sensitivity PA cell based on the Helmholtz Resonator (HR) was designed by the authors (Fig. 1) for air pollution monitoring [2]. This type of resonator consists of two volumes connected by a capillary. The PA HR detector consists of two identical cells equipped with two Knowles electric microphones EK 3027 ($R_m = 0.02 \text{ V Pa}^{-1}$) connected by two identical capillaries (Fig. 2a). Such a design gives the possibility to carry out flow measurements if the differential signal between the microphones is measured. To predict the acoustic properties and sensitivity of

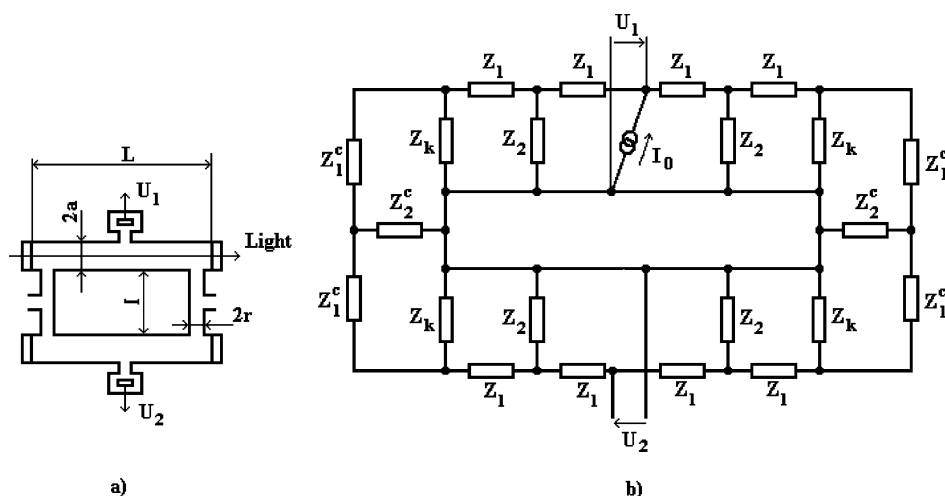


Fig. 2. Schematic representation of the differential Helmholtz resonant (DHR) photoacoustic (PA) cell (a) and its analogous electric line circuit (b).

the PA HR detector, a theoretical model based on acoustic analogy to electric line circuit was used. We have shown in our work that the electric circuit approach is a very efficient method to study acoustic resonance and describe the HR and DHR characteristics with the experimental accuracy [2–4].

3. Prediction of PA DHR frequency response

An acoustic wave in the PA HR cell is generated by absorption of the radiation of a chopped laser beam. Under the assumption that the acoustic wavelength exceeds the overall dimensions of the cell, the corresponding electric line circuit is represented by discrete circuit elements [5]. The pressure amplitude P and volume velocity are replaced in this circuit by the voltage amplitudes U_{m1} , U_{m2} and electric current I_0 . Since the acoustic wave excitation is due to the heat generated by the absorbed power $W_0 \cdot k_v \cdot L$ in the cell, the current source I_0 is expressed as [4]

$$I_0 = \{(\gamma - 1)/(2.22 \cdot \rho \cdot u^2)\} \cdot W_0 \cdot k_v \cdot L, \quad (2)$$

where W_0 is the laser power, k_v is the absorption coefficient of the gas, L is the cell length and u is the sound velocity. The pressure amplitudes U_m ($m = m1, m2$) at the position of the microphones are determined as

$$U_m = Z \cdot I_0 \quad (3)$$

where Z is the acoustic impedance of the acoustic volume (cell).

The potentiality of any PA system is completely determined by such an important parameter as sensitivity $\Lambda = \sqrt{U_n^2}/R$ ($\text{W m}^{-1} \text{Hz}^{-1/2}$), where $\sqrt{U_n^2}$ ($\text{V Hz}^{-1/2}$) is the r.m.s. value of noise, e.g. intrinsic noises of the microphone (Johnson, Brownian, and thermal noises), circuit noise, and external acoustic noise.

When the cell absorption is low ($k_v \cdot L \ll 1$) and the exciting radiation power does not achieve the absorption saturation level, the sensitivity R is a magnitude of the electric signal produced by the microphone for a unit of the power absorbed by molecules per unit length.

The ultimate sensitivity Λ is the noise equivalent power (NEP) of the PA detector defined as the minimum magnitude of the absorbed power, which can be detected at $\text{SNR} = 1$ at a given frequency and a given frequency band.

Sensitive electric microphones are commonly used in measuring low pressure oscillations, and the sensitivity of the PA detector can be presented as the product of the microphone sensitivity R_m and cell sensitivity R_c , $R = R_c \cdot R_m$.

The cell sensitivity is determined as

$$R_c = U_m/W_0 \cdot k_v = Z \cdot \{(\gamma - 1)/(2.22 \cdot \rho \cdot u^2)\} \cdot L. \quad (4)$$

If the acoustic wavelength is comparable with spatial dimensions of the resonator, a longitudinal standing acoustic wave occurs in the cavity. In this case, the modeling by the discrete acoustic impedance fails, and the Helmholtz resonator should be treated in terms of the extended Helmholtz resonator (EHR) theory [6,7]. This approach considers acoustic waves propagation in the cells. The correct impedance of a tube can be calculated by dividing the tube into subcells of infinitesimal length. The connection of the infinitesimal subcells in series yields the characteristic impedance Z_ω and propagation constant γ_ω of an electric transmission line, which describes an acoustic wave propagation through the tube. The retransformation of an electric transmission line into a simple circuit consisting of discrete acoustic elements Z_i yields the electric line circuit of the EHR (Fig. 2b).

Expressions for calculation of the characteristic impedances Z_ω and Z_ω^c , propagation constants γ_ω and γ_ω^c , and discrete acoustic impedances Z_i and Z_i^c are given in Ref. [7]

$$Z_\omega = \frac{\rho u}{\pi a^2} \left[\frac{1 + \frac{d_v}{a}}{1 + (\gamma - 1) \frac{d_t}{a}} \right]^{1/2} \times \left[1 - \frac{i}{2} \left(\frac{\gamma - 1}{\frac{a}{d_v} + 1} - \frac{\gamma - 1}{\frac{a}{d_t} + (\gamma - 1)} \right) \right];$$

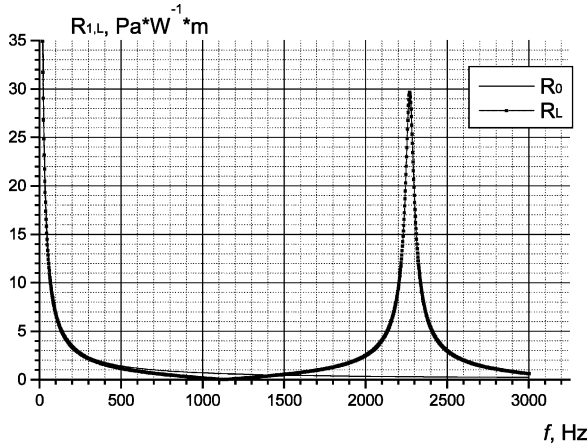


Fig. 3. Calculated cell sensitivity of non-resonant R_0 and longitudinal resonant R_L cells vs. modulation frequency f . Cell pressure is one atmosphere.

$$\gamma_\omega = \frac{i\omega}{u} \left[\left(1 + \frac{d_v}{a} \right) \left(1 + (\gamma - 1) \frac{d_t}{a} \right) \right]^{1/2} \times \left[1 - \frac{i}{2} \left(\frac{\gamma - 1}{\frac{a}{d_t} + (\gamma - 1)} + \frac{1}{a/d_v} \right) \right]; \quad (5)$$

$$Z_1 = Z_\omega \tanh\left(\frac{\gamma_\omega L}{4}\right) \quad \text{and} \quad Z_2 = \frac{Z_\omega}{\sinh\left(\frac{\gamma_\omega L}{2}\right)};$$

$$Z_\omega^c = \frac{\rho u^2}{\pi r^2} \left[\frac{1 + \frac{d_v}{r}}{1 + (\gamma - 1) \frac{d_t}{r}} \right]^{1/2} \times \left[1 - \frac{i}{2} \left(\frac{\gamma - 1}{\frac{r}{d_v} + 1} - \frac{\gamma - 1}{\frac{r}{d_t} + (\gamma - 1)} \right) \right];$$

$$\gamma_\omega^c = \frac{i\omega}{u} \left[\left(1 + \frac{d_v}{r} \right) \left(1 + (\gamma - 1) \frac{d_t}{r} \right) \right]^{1/2} \times \left[1 - \frac{i}{2} \left(\frac{\gamma - 1}{\frac{r}{d_t} + (\gamma - 1)} + \frac{1}{r/d_v} \right) \right]; \quad (6)$$

$$Z_1^c = Z_\omega^c \tanh\left(\frac{\gamma_\omega^c L}{2}\right) \quad \text{and} \quad Z_2^c = \frac{Z_\omega^c}{\sinh(\gamma_\omega^c L)};$$

$$Z_k \rightarrow \infty \quad \text{close cell}$$

$$Z_k \rightarrow 0 \quad \text{open cell} \quad (7)$$

Here $\omega = 2\pi f$ is the circular modulation frequency of laser beam, ρ is the gas density, $\gamma = C_p/C_v$ is the ratio of specific heats at constant pressure and volume, and U_{m1} and U_{m2} are signal amplitudes of the microphones.

The thicknesses d_v and d_t of the viscous and thermal boundary layers of the cell and capillary walls are described by the expressions

$$d_v = \sqrt{\frac{2\mu}{\rho \cdot \omega}}; \quad (8)$$

$$d_t = \sqrt{\frac{2K}{\rho \cdot \omega \cdot c_p}}; \quad (9)$$

where μ is the viscosity and K is the heat conductivity of buffer gas.

Calculated according to expression (4), the sensitivities versus modulation frequency f of nonresonant and longitudinal resonant cells are shown in Fig. 3.

The acoustic impedances of nonresonant Z_0 and resonant Z_l cells are defined as follows

$$Z_0 = \frac{1}{iC2\pi f} \quad C = \frac{V}{\rho u^2}; \quad (10)$$

$$Z_l = \frac{1}{2} \left[Z_1 + \frac{Z_2(Z_1 + Z_k)}{Z_1 + Z_2 + Z_k} \right]; \quad (11)$$

where $V = \pi a^2 l$ is the cell volume; Z_1 , Z_2 , and Z_k are calculated by Eqs. (5) and (7).

Fig. 4 presents the calculated sensitivities vs. modulation frequency f for DHR cell (Figs. 1 and 2). Table 1 lists specifications for DHR cell and the buffer gas N_2 at the atmospheric pressure.

Table 1
Specifications for DHR cell and buffer gas N_2

Cell length L (m)	0.150
Cell radius a (m)	0.0036
Capillary length l (m)	0.0984
Capillary radius r (m)	0.0030
Mass density ρ (kg m^{-3})	1.1662
Sound velocity u (m s^{-1})	346
Thermal conductivity k ($\text{W m}^{-1} \text{K}^{-1}$)	0.02598
Specific heat capacity C_v ($\text{J kg}^{-1} \text{K}^{-1}$)	718
$\gamma = C_p/C_v$	1.4
Viscosity μ ($\text{kg m}^{-1} \text{s}^{-1}$)	1.79×10^{-5}

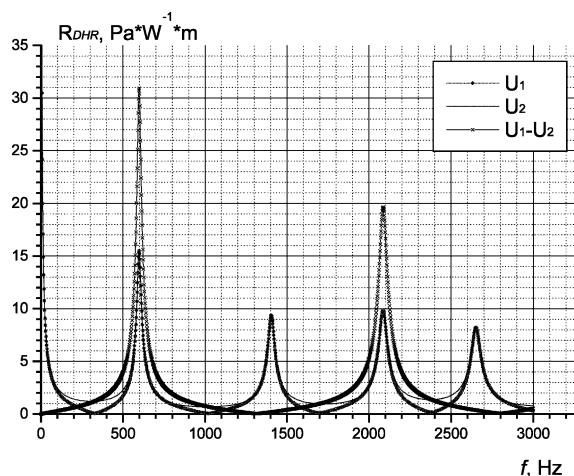


Fig. 4. Calculated cell sensitivity of DHR cell R_{DHR} vs. modulation frequency f . Cell pressure is one atmosphere.

At the atmospheric pressure the sensitivity R_{DHR} of the PA cell slightly exceeds the sensitivity R_L of the PA cell with longitudinal resonance.

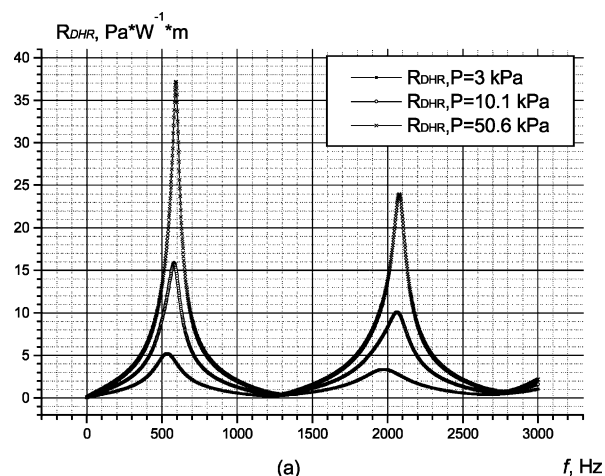
As has been shown [2–4], due to recording the difference between the signals from microphones located in different DHR cells and subtraction of in-phase external noises, the r.m.s. noise value for the DHR cell is lower than that for non-resonant and longitudinal resonant PA cells and, correspondingly, the ultimate sensitivity Λ is 1–2 orders of magnitude lower. This is of particular importance in the regime of continuous gas flow through the PA cell.

Within the pressure region 1–101.3 kPa, the gas elasticity significantly changes. Since such thermodynamic characteristics of the medium as viscosity, heat conductivity, heat capacity, adiabatic exponent, and sound velocity only slightly depend on the pressure, the magnitude of the sensitivity $R_{DHR}(f)$ and the value of the resonance frequency f_0 are determined by the pressure and temperature dependence of the medium density

$$\rho = \frac{m}{RT} P, \quad (12)$$

where m is the molar mass, R is the gas constant, P is the buffer gas pressure, and T is the gas temperature.

Fig. 5a presents the frequency dependence of



(a)

(b)

(c)

(d)

(e)

(f)

(g)

(h)

(i)

(j)

(k)

(l)

(m)

(n)

(o)

(p)

(q)

(r)

(s)

(t)

(u)

(v)

(w)

(x)

(y)

(z)

Fig. 5. Calculated cell sensitivity of DHR cell R_{DHR} vs. modulation frequency f at different pressures in the cell (a) and sensitivities of longitudinal resonant R_L , Helmholtz R_1 and differential Helmholtz resonant R_{DHR} cells at reduced pressure ($P = 3$ kPa) (b).

the sensitivity R_{DHR} calculated for reduced pressures. Decrease of gas pressure in the DHR cell from 50.6 to 3 kPa results in significant (6-fold) decrease of the sensitivity $R_{DHR}(f_0)$ and 10% change of resonance frequency. At the same time, up to 3 kPa, inclusive, the peculiarities of the Helmholtz resonance (Fig. 5b) and phase opposition of pressure oscillations within different cells remain invariable; the DHR cell sensitivity therein is twice higher than that of the HR cell and five times higher than the sensitivity of some isolated cell.

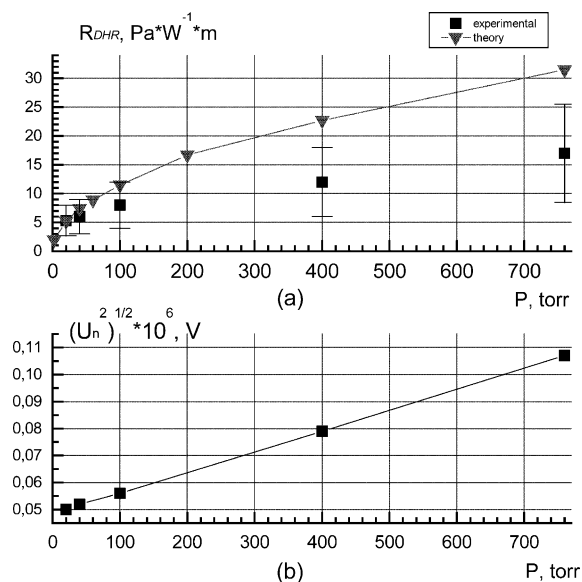


Fig. 6. Sensitivity R_{DHR} (a), r.m.s. noise level $\sqrt{U_n^2}$ (b) vs. cell pressure.

4. Application of the DHR to water vapor detection

Measurements of the sensitivity R_{DHR} and ultimate sensitivity Λ_{DHR} of the PA DHR detector at atmospheric and reduced pressures were conducted using the PA-spectrometer with near IR diode laser.

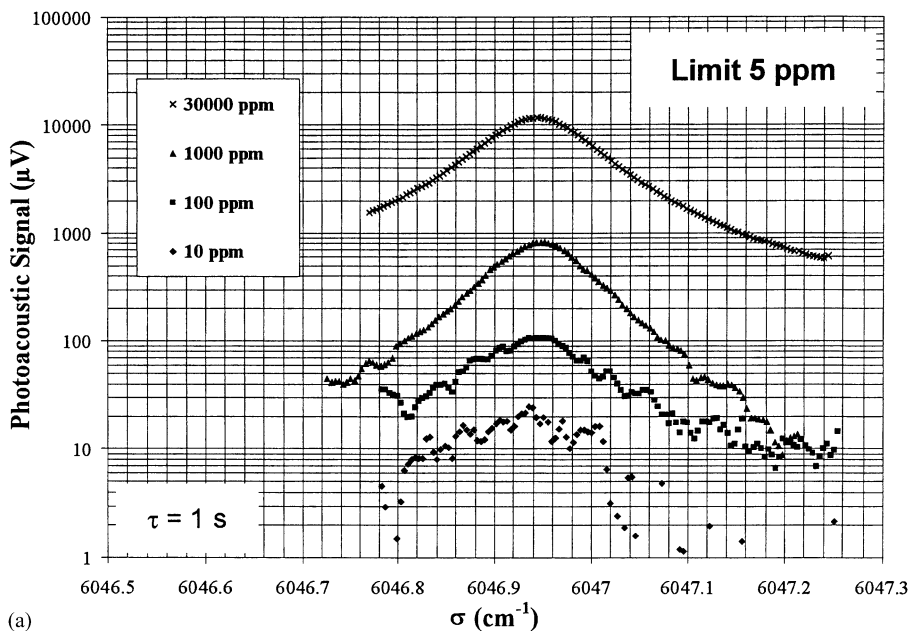
The vacuum system allows measurements of the PA detector characteristics under flow and flowless operation modes. The flow operation mode (continuous blowing of gas through the measurement cell) at atmospheric and reduced pressures was made with the use of two volume-controllable capillaries (1×10^{-6} – 1.33×10^{-4} m^3 kPa s^{-1}). The pressure at the cell input was measured with the vacuum manometer MKS Baratron type 127.

To determine the sensitivity and ultimate sensitivity of the PA DHR detector, the absorption coefficient of the well-known H_2O absorption line ($\nu_0 = 12496.1056$ cm^{-1} ; $\gamma_L = 0.103$ cm^{-1} ; $S = 0.58 \times 10^{-4}$ cm^{-2} atm^{-1} ; $\gamma_D = 0.018$ cm^{-1} ; $T = 296$ K) was measured. The H_2O absorption line shape was obtained at the mean power of the diode laser of 5.4 mW. Each absorption line was

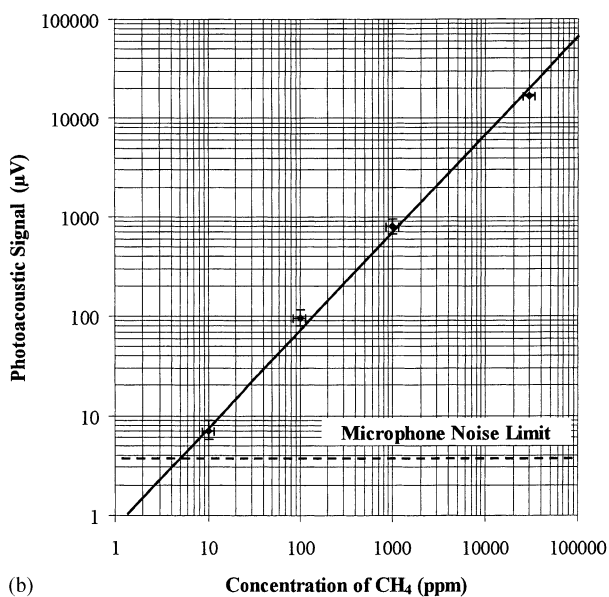
Table 2

Three configurations of DHR cell and application to methane detection at atmospheric pressure

	1st cell	2nd cell	3rd cell
<i>Mechanical characteristics</i>			
Cell length L_c (m)	0.1	0.1	0.1
Cell radius R_c (m)	0.005	0.005	0.005
Capillary length L_{cap} (m)	0.1	0.1	0.1
Capillary radius R_{cap} (m)	0.001	0.001	0.002
<i>Acoustical characteristics</i>			
Microphone	Knowles	Sennheiser	Bruel & Kjaer
Microphone model	EK1024	KE4	BK4144
Microphone sensitivity (mV Pa^{-1})	15.8	10	45
Λ ($\text{W m}^{-1} \text{Hz}^{-1/2}$)	1.9×10^{-6}	1.5×10^{-6}	1.2×10^{-7}
<i>Methane application</i>			
Absorption band	$2\nu_3$	$2\nu_3$	$2\nu_3$
Absorption lines	R(7)	R(3)	R(3)
Wavenumber (cm^{-1})	6087	6047	6047
Laser diode	IBSG	SU	SU
Diode modulated power W (W)	2×10^{-4}	7×10^{-4}	7×10^{-4}
Absorption coefficient K (m^{-1})	32	35	35
α_{min} (m^{-1}) = Λ/W	0.0097	0.0021	0.00017
c_{min} (ppm) = α_{min}/K	300	60	5



(a)



(b)

Fig. 7. Photoacoustic (PA) signal vs. wavenumber at different methane concentration in 1 atmosphere of N_2 with an integration time of 1 s (a) and PA signal vs. methane concentration (b).

approximated by the Voigt contour, and the values of the r.m.s. intensity of noises and amplitude of difference between the microphones' signals were found from this fitting.

Fig. 6a,b presents the dependences of the signal

sensitivity and noise levels on pressure both experimental and calculated by Eq. (4).

Estimation of the DHR cell sensitivity was made assuming that the microphone sensitivity R_m is independent of pressure. Nevertheless, as

shown in Refs. [2–4], it always increases as the pressure falls. On the one hand, this leads to overestimation of the cell sensitivity, on the other, taking into account the decrease of noise level (Fig. 6b), this results in very weak pressure dependence of the ultimate sensitivity of the PA DHR detector. Suppression of the external acoustic noise caused by continuous gas flow through the PA cell of DHR detector at atmospheric pressure and flow rate of 0.5 l min^{-1} has been demonstrated in Ref. [2].

5. Application to methane detection at atmospheric pressure

The DHR was used in conjunction with an IBSG (St. Petersburg, Russia) multimode diode laser and a Sensor Unlimited (USA) DFB diode laser to demonstrate methane detection at atmospheric pressure. Methane was excited in the $2\nu_3$ band at $1.65 \mu\text{m}$. We designed three cells with different radius of the capillary and equipped with different commercial microphones.

Table 2 summarises the mechanical and acoustical characteristics of our cells and the application to methane. The improvements in microphones, design and diode lasers have permitted to decrease the obtained minimal de-

tectable concentration given in the last row: 300, 60 and then 5 ppm.

The observed diode laser spectra is recorded while varying the diode laser current (i.e. the wavelength) for different concentrations of methane in 1 atmosphere of N_2 for the last described cell (Fig. 7a). The PA signal for the maximum absorption is reported vs. the methane concentration (Fig. 7b). We demonstrate here the linearity of the method. The crossing between this line and the microphone noise sensitivity give the detection limit of 5 ppm for this experiment as given in the third column of Table 2.

References

- [1] M.W. Sigrist, *Air Monitoring by Spectroscopic Techniques*, Wiley, New York, 1994.
- [2] V. Zéninari, V.A. Kapitanov, D. Courtois, Yu.N. Ponomarev, *Infrared Phys. Technol.* 40 (1999) 1.
- [3] A.B. Antipov, V.A. Kapitanov, Yu.N. Ponomarev, V.H. Sapozhnikova, *Optoacoustic Method in Laser Molecular Spectroscopy*, Nauka, Novosibirsk, 1984, p. 280.
- [4] Yu.N. Ponomarev, B.G. Ageev, M.W. Sigrist, V.A. Kapitanov, D. Courtois, O.Yu. Nikiforova, *Laser optoacoustic spectroscopy of intermolecular interaction in gases*, SSI RASKO, 2000, p. 200.
- [5] O. Nordhaus, J. Pelzl, *Appl. Phys.* 25 (1981) 221.
- [6] J. Pelzl, K. Klein, O. Nordhaus, *Appl. Optics* 21 (1982) 94.
- [7] R. Kastle, M.W. Sigrist, *Appl. Phys. B* 63 (1996) 389.